R. & M. No. 2551
(6059)
A.R.C. Technical Report

MINISTRY OF SUPPLY

AERONAUTICAL RESEARCH COUNCIL
REPORTS AND MEMORANDA

Graphical Treatment of Binary Mass-balancing Problems

By

R. A. FRAZER, B.A., D.Sc.,
of the Aerodynamics Division, N.P.L.

LONDON: HIS MAJESTY'S STATIONERY OFFICE
1951
TWO SHILLINGS NET

Graphical Treatment of Binary Mass-balancing Problems

By

R. A. FRAZER, B.A., D.Sc., of the Aerodynamics Division, N.P.L.

Reports and Memoranda No. 2551

28*th August,* 1942

Summary.—A graphical method, based on 'classical' flutter theory, is described which provides a simple test of the effectiveness of mass-balancing in the prevention of flutter at various heights. Illustrative applications are made to flexural-aileron and servo-rudder flutter. It is suggested that diagrams of this type may be a useful aid in design.

1. *Purpose of the Investigation.*—In A.R.C. Report No. 5668[1] the greatest length of balancing arm which is effective in the prevention of certain types of binary flutter is deduced from stability diagrams calculated by vortex strip theory. The present paper shows that similar diagrams can be derived simply by classical flutter theory and known properties of test conics[2].

The diagram, which is illustrated for flexural-aileron flutter and servo-rudder flutter by Figs. 3 and 6, indicates immediately whether a proposed modification of the masses from any given inertial condition of the system will be effective in the absolute prevention of flutter at any given height. The abscissa and the ordinate are, respectively, the product of inertia coefficient and the moment of inertia coefficient of the flap; and the diagram consists essentially of a curve B_u (stability boundary) which depends solely on the aerodynamic coefficients. This curve separates the diagram into 'safe' and 'unsafe' regions. Flutter is prevented absolutely for all inertia values which plot within the safe region.

It is suggested that the preparation of diagrams of this type appropriate to standard types of flutter and standard types of aircraft would be a useful aid in design.

2. *Flexural-aileron Mass-balancing Diagram.*—The basic formulae required are given in Chapters 3 and 8 of R. & M. 1155[2], but the definitions of the non-dimensional dynamical coefficients are modified in Table 1 below to accord with modern notation[1]. The root chord of the wing is denoted by c_0, and the reference section is assumed to lie at distance l from the root.

TABLE 1

Coefficients for Flexural-aileron Motion

Flexural Moments			Aileron-hinge Moments		
Coefficient	Significance	Non-dimensional Form	Coefficient	Significance	Non-dimensional Form
A_1	Inertia	$\rho l^3 c_0{}^2 a_1$	P	Inertia	$\rho l^2 c_0{}^3 p$
B_1	$-L_{\dot\phi}$	$\rho V l^3 c_0 b_1$	B_2	$-H_{\dot\phi}$	$\rho V l^2 c_0{}^2 b_2$
C_1	l_ϕ	$\rho V^2 l^3 \left(\frac{l_\phi}{\rho V^2 l^3}\right)$	C_2	0	0
P	Inertia	$\rho l^2 c_0{}^3 p$	D_2	Inertia	$\rho l c_0{}^4 d_2$
E_1	$-L_{\dot\xi}$	$\rho V l^2 c_0{}^2 e_1$	E_2	$-H_{\dot\xi}$	$\rho V l c_0{}^3 e_2$
F_1	$-L_\xi$	$\rho V^2 l^2 c_0 f_1$	F_2	$h_\xi - H_\xi$	$\rho V^2 l c_0{}^2 \left(\frac{h_\xi}{\rho V^2 l c_0{}^2} + f_2\right)$

(93005) A

Supplementary symbols required are :—

$$X \equiv l_\phi/\rho V^2 l^3 ; \quad V \equiv (h_\xi/\rho V^2 l c_0^2) + f_2 ;$$

$$|be| \equiv b_1 e_2 - b_2 e_1 ; \quad |bf| \equiv b_1 f_2 - b_2 f_1 ;$$

$$\alpha \equiv |be| - p f_1 ; \quad \beta \equiv b_2 f_1 ;$$

$$q_1 \equiv a_1 e_2 + d_2 b_1 - p(e_1 + b_2) ; \quad \Delta \equiv 4 b_1 e_2 - (e_1 + b_2)^2 :$$

The inertial coefficients can be defined as follows. Let m denote the element of mass at distance y from the wing root and at distance $c_0\xi$ behind the aileron hinge axis. Also let f_y denote the ratio of the linear bending displacement of the wing at distance y from the wing root to the corresponding displacement at the reference section. Then

$$a_1 = \sum_{\mathrm{w}} m f_y^2/\rho l c_0^2 ; \quad p = \sum_{\mathrm{a}} m \xi f_y/\rho l c_0^2 ; \quad d_2 = \sum_{\mathrm{a}} m \xi^2/\rho l c_0^2 , \qquad \ldots \quad \ldots \quad (1)$$

where $\sum_{\mathrm{w}}$ denotes summation over the complete wing and $\sum_{\mathrm{a}}$ denotes summation over the aileron only.

Some possible types of test-conic appropriate to flexural-aileron flutter are shown in Fig. 1. In each case the stiffness point Z has the co-ordinates $(0, f_2)$, and the points of intersection of the conic with both co-ordinate axes are real. Two of these points M, N, are independent of inertias, and are given by $OM = \beta/b_1$, $ON = \beta/e_2$. Thus

$$OZ - OM = \frac{|bf|}{b_1} .$$

On the other hand the positions of the other two intersections M', N', depend on the inertias.

With symmetrical flutter the slope of the stiffness line ZP is proportional to the stiffness ratio h_ξ/l_ϕ, and with anti-symmetrical flutter ZP' is parallel to OX. Since h_ξ—the stiffness of the control circuit—may be subject to some variation in practice even on aircraft of a given type, the ideal safeguard is *absolute* prevention of flutter. The conic must then be so disposed that real intersections with all stiffness lines are avoided.

The first essential condition for absolute prevention of flutter is that Z shall lie above M. This requires

$$|bf| > 0 , \qquad \ldots \quad \ldots \quad \ldots \quad \ldots \quad \ldots \quad \ldots \quad (2)$$

which inequality will be assumed to be satisfied. Flutter is then certainly prevented absolutely provided the maximum ordinate $Y_{\max}$ of the conic does not exceed OZ. This restriction is sufficient but not necessary, as is obvious, for example, from Figs. 1 (c) and (d). The restriction will, however, first be imposed and later relaxed.

Now the two stationary ordinates of the conic are given by*

$$S(Y, p, d_2) \equiv Y^2 p^2 \Delta - 2Y \{2 e_2 \beta p^2 + p(e_1 + b_2)(\alpha e_2 - \beta d_2) - 2 b_1 e_2 \alpha d_2\}$$
$$- (\alpha e_2 + \beta d_2)^2 = 0 , \quad \ldots \quad \ldots \quad \ldots \quad \ldots \quad \ldots \quad \ldots \quad (3)$$

and the positive root corresponds to $Y_{\max}$. Thus $Y_{\max}$ is independent of a_1, and the critical pairs of values of p and d_2 separating the cases $Y_{\max} > f_2$ and $Y_{\max} < f_2$ are given by the condition

$$S(f_2, p, d_2) = 0 . \qquad \ldots \quad \ldots \quad \ldots \quad \ldots \quad \ldots \quad (4)$$

Values of p and d_2 which render $S(f_2, p, d_2) < 0$ correspond to the cases $Y_{\max} > f_2$. For example, when d_2 is very large, $S(f_2, p, d_2) < 0$ and by (3) $Y_{\max}$ is then also large.

*Equation (3) is deducible from (152) of R. & M. 1155[2] by appropriate changes of the symbols.

Equation (4) represents a conic section in the plane of (p, d_2) which depends solely on the aerodynamic coefficients. The equation to the curve is expressible as

$$A_0\xi^2 + 2H_0\xi\eta + B_0\eta^2 + 2G_0\xi + 2F_0\eta - 1 = 0\,, \qquad (5)$$

where $\xi \equiv p/e_2|be|$; $\eta \equiv d_2/e_2|be|$,

and

$$\begin{aligned} A_0 &= \Delta f_2^2 + 2e_2(e_1 - b_2) f_1 f_2 - e_2^2 f_1^2, \\ 2H_0 &= 2\{b_2(e_1 + b_2) - 2b_1 e_2\} f_1 f_2 + 2e_2 b_2 f_1^2, \\ B_0 &= -b_2^2 f_1^2, \\ 2G_0 &= 2e_2 f_1 - 2(e_1 + b_2) f_2, \\ 2F_0 &= -2b_2 f_1 + 4b_1 f_2\,. \end{aligned}$$

It is found that

$$\Delta_0 \equiv H_0^2 - A_0 B_0 = 4e_2|bf|\,|be| f_1^2 f_2\,, \qquad (6)$$

which is positive in view of (2) and the known condition $|be| > 0$. Hence the conic (5) is hyperbolic. The centre, say (p_c, d_{2c}), is given by

$$\left.\begin{aligned} 2f_1 p_c &= 2b_1 e_2 - b_2(e_1 + b_2) \\ 2f_1^2 d_{2c} &= e_2(e_1 - b_2) f_1 + \Delta f_2 \end{aligned}\right\}, \qquad (7)$$

and the asymptotes are parallel to

$$(H_0 \pm \sqrt{\Delta_0})\, p = b_2^2 f_1^2 d_2\,. \qquad (8)$$

The two intercepts on the axis $p = 0$ are positive, and are given by

$$f_1^2 b_2^2 d_2/e_2|be| = (\sqrt{|bf|} \pm \sqrt{(b_1 f_2)})^2\,, \qquad (9)$$

while the intercepts on $d_2 = 0$ are given by

$$A_0 p/e_2|be| = -e_2 f_1 + (e_1 + b_2) f_2 \pm 2\sqrt{(e_2 f_2 |bf|)}\,. \qquad (10)$$

In Fig. 2 the upper and lower branches of the hyperbola are respectively marked B_u, B_l, and the region lying above B_u (shown shaded) is termed 'unsafe'. Points in that region, and points in the region below B_l, correspond to the condition $Y_{\max} > f_2$: whereas points lying between B_u and B_l correspond to $Y_{\max} < f_2$, and thus to cases in which flutter is certainly prevented absolutely. It will now be shown that flutter is also certainly prevented for all points below B_l, so that B_u can be regarded as the effective 'stability boundary'.

Let MM_1 in Fig. 1 be the chord of the test conic drawn through M parallel to OX. Then it is readily shown that

$$X_{M1} = -q_1\left\{\frac{\beta p}{b_1}(e_1 + b_2) + \alpha e_2 - \beta d_2\right\}\Big/ A\,,$$

where $A \equiv e_2\{b_1 d_2^2 - p d_2(e_1 + b_2) + e_2 p^2\}$. Now q_1 and A are known to be both positive. Hence M_1 lies to the right or to the left of M according as

$$W(p, d_2) \equiv \frac{\beta p}{b_1}(e_1 + b_2) + \alpha e_2 - \beta d_2 < 0 \text{ or } > 0\,.$$

When $W(p, d_2) = 0$, M and M_1 are coincident. In this case the tangent at M is horizontal, so that $Y_{\max} = OM < f_2$. It follows that if the straight line $W(p, d_2) = 0$ were plotted in Fig. 2, this locus would lie wholly between the branches B_u and B_l. Moreover, all points below the line (whether above or below B_l) would yield test conics satisfying the condition $X_{M1} < 0$. But from Fig. 1 (c) it is clear that when the conic is such that $X_{M1} < 0$, flutter is prevented even when $Y_{\max} > f_2$; that is to say, even for points in Fig. 2 situated below the branch B_l. The whole of the region below B_u may accordingly be classed as safe.

From the preceding discussion it does not follow that all parts of the region *above* B_u are necessarily to be classed as unsafe. In fact, while it is true that for any point of that region $Y_{\max} > f_2$ and $X_{M1} > 0$, yet flutter would be prevented absolutely if the conic happened to be as shown in Fig. 1(d). The characteristics of such a conic are

(*a*) $OZ \geqslant OM' \geqslant OM$,

(*b*) $\dfrac{dY}{dX} < 0$ at M',

(*c*) $Y_{\max} > f_2$.

The discussion of these conditions is complicated and will be omitted. It can be shown that conditions (*a*) certainly cannot be satisfied unless $\alpha < 0$ (*i.e.*, unless $P \geqslant |be|/f_1$), and that a_1 must then lie between the bounds

$$- b_1\alpha/\beta \geqslant a_1 \geqslant - \alpha/f_2.$$

Moreover, the slope of the tangent at M is given by

$$\frac{B}{q_1^2}\left(\frac{dY}{dX}\right)_{M'} = \frac{OM'}{OM' - OM} - \frac{b_1 A}{e_2 q_1^2},$$

from which it follows that condition (*b*) certainly cannot be satisfied when M' is close to M. These considerations indicate that a conic of the type Fig. 1(d) cannot arise without severe, if not quite impracticable, restrictions on the values of all three inertial coefficients a_1, p and d_2. Hence any possible extension of the safe region would merely cover very exceptional inertial conditions of the system, and would destroy the attractive simplicity of the diagram.

The application to the problem of mass-balancing will now be considered. In Fig. 2 J_0 is the inertia point corresponding to a datum mass distribution and to a datum air density ρ_0 (*e.g.*, 0·002378, at sea-level). If J_0 falls within the safe region flutter is already prevented absolutely for $\rho = \rho_0$. Suppose, on the other hand, that J_0 falls within the unsafe region, as shown in Fig. 2. Then if a mass m is added to the aileron at distance k from the wing root and at distance λc_0 *forward* of the hinge axis, the changes of the co-ordinates of J are (*see* (1))

$$\delta p = - m\lambda f_k/\rho_0 l c_0^2; \qquad \delta d_2 = m\lambda^2/\rho_0 l c_0^2 . \qquad \ldots \qquad (11)$$

The diagram tests immediately whether the new inertia point, say J_1, lies in the safe region, as required. The optimum mass modification in any given case will of course depend very largely on the practical restrictions to the length of the balancing arm. It may be noted here that no point J_0 can be brought from the unsafe to the safe region unless the gradient λ/f_k of the line J_0J_1 is numerically less than the gradient of the steeper asymptote LL (*see* (8)). Thus, theoretically, there exists a maximum permissible length of balancing arm in each wing section, which depends solely on the aerodynamic coefficients and is independent of altitude. A numerical example given later indicates that, when the aileron is hinged near its leading edge, the critical length of arm is very great.

For flight at heights other than sea-level the datum values of the inertias require to be multiplied by the factor ρ_0/ρ. Representative values[3] of this factor are as follows.

Altitude (ft)	0	10,000	20,000	30,000	40,000
Factor ρ_0/ρ	1·0	1·35	1·88	2·67	4·06

With a diagram of the type shown in Fig. 2 an increase of altitude *without alteration* of k, λ, and m, will displace both J_0 and J_1 outwards along the radii through O to, say, J_0' and J_1'; also $J_0'J_1'$ will remain parallel to J_0J_1. Hence, as the height increases J_1' tends to approach, or recede from, the unsafe region according as OJ_1 is steeper, or less steep, than the asymptote LL. In particular, if static balance is applied, OJ_1 will coincide with the axis of d_2, and the maximum safe flying height will be given by the condition* $d_2 = OV$. It follows also that, unless considerable mass-overbalance is applied, any remedial mass modification should be based on the maximum flying height.

An approximation to the diagram which errs on the safe side and probably covers practical requirements, is obtained by replacing the hyperbolic branch B_u by the asymptote LL. When the aileron is hinged near its leading edge the coefficient H_0 in (8) will be negative, and the equation to LL then is

$$(p - p_c)\,(H_0 - \sqrt{\Delta_0}) = b_2^2 f_1^2\,(d_2 - d_{2c})\,,$$

Where p_c, d_{2c} are given by (7).

Numerical Example.—Fig. 3 shows the diagram calculated for a fighter aircraft with the use of rough data. The values adopted for the aerodynamic coefficients were derived by approximations to the air-load coefficients calculated in A.R.C. 5668[1], and are

$$b_1 = 5\cdot78\,; \qquad e_1 = 0\cdot298\,; \qquad f_1 = 1\cdot39\,;$$

$$b_2 = 0\cdot00972\,; \qquad e_2 = 0\cdot009225\,; \qquad f_2 = 0\cdot0146\,.$$

The reference section is chosen at the section $l = 0\cdot57s$ (inboard end of aileron). Also it is assumed that for full-scale $c_0 = 5\cdot87$ ft and c_a (aileron chord) $= 0\cdot235c_0$.

The equation to the hyperbola (5) works out as

$$-\,144\cdot2p^2 - 1784pd_2 - 843\cdot6d_2^2 + 35\cdot82p + 667\cdot6d_2 - 1 = 0$$

The centre is at $p_c = 0\cdot0373$, $d_{2c} = 0\cdot00140_5$, and the slopes of the two asymptotes are $-\,21\cdot14$ and $-\,0\cdot0081$. In this case the limiting length for a balancing arm fitted in the reference section ($f_k = 1$) is given by $\lambda = 21\cdot14$, and is thus of the order 20 wing chords.

Values given in A.R.C. 5668 for the structural inertial coefficients appropriate to sea-level, without any mass-balance applied, are as follows.

Fabric-covered aileron	$p = 0\cdot0836$,	$d_2 = 0\cdot00533$,
Aluminium-covered aileron	$p = 0\cdot309$,	$d_2 = 0\cdot0197$.

When the aileron is *uniformly* statically balanced (*i.e.*, $p = 0$, with centre of mass on hinge axis in every section), the values of d_2 are $0\cdot0107$ and $0\cdot0395$ for fabric and aluminium respectively.

The situations of some representative inertia points are indicated in Fig. 3. Points marked F, A, refer respectively to the fabric and the aluminium covering. The intercept OV of the stability boundary on the axis of d_2 is about $0\cdot79$ and is well beyond the limits of the diagram. Uniform static balance would thus be effective in preventing flutter of the aluminium-covered aileron at all practical flying heights.

3. *Aileron-spring-tab and Servo-rudder Diagrams.*—A simple discussion of these two types of binary flutter on the basis of classical derivative theory and without the use of non-dimensional coefficients is given in section 10 of A.R.C. 5668[1]. The theory is similar to that for torsional-aileron flutter, except that 'barred' dynamical coefficients are introduced in order to eliminate the elastic cross-stiffness. The barred coefficients, in general, depend upon two positive geometrical constants n and N subject to the restriction $N > n$. With the normal type of servo-rudder $n = 0$. The dynamical coefficients appropriate to standard air density (flight at sea-level) are as defined in Tables 2 and 3. For flight at other heights the inertial and elastic coefficients require to be multiplied by the factor ρ_0/ρ.

---

* OV is given by (10) with the positive sign for the radical.

TABLE 2

Unbarred Dynamical Coefficients

Tab or Servo Hinge Moments T			Aileron or Rudder Hinge Moments H		
Coefficient	Significance	Equivalent	Coefficient	Significance	Equivalent
D_2	Inertia ..	d_2	P	Inertia ..	p
E_2	$-T_\beta$ ..	e_2V	E_3	$-H_\beta$ ..	e_3V
F_2	$t_\beta - T_\beta$ ..	$t_\beta + f_2V^2$	F_3	$h_\beta - H_\beta$ ..	$h_\xi + f_3V^2$
P	Inertia ..	p	G_3	Inertia ..	g_3
J_2	$-T_\xi$ ..	j_2V	J_3	$-H_\xi$ ..	j_3V
K_2	$t_\xi - T_\xi$ ..	$t_\xi + k_2V^2$	K_3	$h_\xi - H_\xi$ ..	$h_\xi + k_3V^2$

TABLE 3

Barred Dynamical Coefficients

New Coefficient	Value in Terms of Original Coefficient	New Coefficient	Value in Terms of Original Coefficient
$\bar{d}_2$	$d_2\mathrm{N}^2 + 2p\mathrm{N} + g_3$	$\bar{p}$	$d_2n\mathrm{N} + p(n + \mathrm{N}) + g_3$
$\bar{e}_2$	$e_2\mathrm{N}^2 + (j_2 + e_3)\mathrm{N} + j_3$	$\bar{e}_3$	$e_2n\mathrm{N} + j_2n + e_3\mathrm{N} + j_3$
$\bar{f}_2$	$f_2\mathrm{N}^2 + (k_2 + f_3)\mathrm{N} + k_3$	$\bar{f}_3$	$f_2n\mathrm{N} + k_2n + f_3\mathrm{N} + k_3$
$\bar{p}$	$d_2n\mathrm{N} + p(\mathrm{N} + n) + g_3$	$\bar{g}_3$	$d_2n^2 + 2pn + g_3$
$\bar{j}_2$	$e_2n\mathrm{N} + j_2\mathrm{N} + e_3n + j_3$	$\bar{j}_3$	$e_2n^2 + (j_2 + e_3)n + j_3$
$\bar{k}_2$	$f_2n\mathrm{N} + k_2\mathrm{N} + f_3n + k_3$	$\bar{k}_3$	$f_2n^2 + (k_2 + f_3)n + k_3$
$\bar{t}_\beta$	$t_\beta\mathrm{N}^2 + 2h_\beta\mathrm{N} + h_\xi$	$\bar{h}_\beta$	0
$\bar{t}_\xi$	0	$\bar{h}_\xi$	$t_\beta n^2 + 2h_\beta n + h_\xi$

Other symbols required are:

$$X = (\bar{t}_\beta/V^2) + \bar{f}_2; \qquad Y = (\bar{h}_\xi/V^2) + \bar{k}_3;$$

$$\beta = \bar{j}_2\bar{f}_3 + \bar{e}_3\bar{k}_2; \qquad \Omega = +\sqrt{(\beta^2 - 4\bar{e}_2\bar{j}_3\bar{k}_2\bar{f}_3)};$$

$$\alpha = (\bar{e}_2\bar{j}_3 - \bar{e}_3\bar{j}_2) - \bar{p}(\bar{k}_2 + \bar{f}_3);$$

$$q_1 = \bar{d}_2\bar{j}_3 \quad \bar{g}_3\bar{e}_2) - \bar{p}(\bar{j}_2 + \bar{e}_3);$$

$$\triangle = 4\bar{e}_2\bar{j}_3 - (\bar{j}_2 + \bar{e}_3)^2 = (\mathrm{N} - n)^2\{4e_2j_3 - (j_2 + e_3)^2\}.$$

It is assumed that the test conic appropriate to the barred coefficients is elliptic ($\triangle > 0$). The common intersections of the ellipse, the frequency line, and the divergence hyperbolic $XY = \bar{f}_2\bar{k}_3$, are given by*

$$2\bar{j}_3X_M = \beta - \Omega; \qquad 2\bar{j}_3X_N = \beta + \Omega;$$

$$2\bar{e}_2Y_M = \beta + \Omega; \qquad 2\bar{e}_2Y_N = \beta - \Omega.$$

From numerical examples it appears that in normal practical cases the points M, N will be real, and that the stiffness point $Z(\bar{f}_2, \bar{k}_3)$ will lie above the frequency line MN and to the right of N, as shown in Fig. 4. Flutter will then certainly be prevented if $X_{\mathrm{max.}}$, the maximum abscissa of

* *See* equations (142a) and (142b) of R. & M. 1155.

the ellipse, does not exceed $\bar{f}_2$. The equation* giving $X_{\max.}$ is similar to (3), but contains some additional terms: thus

$$\begin{aligned} S(X, \bar{p}, \bar{d}_2) &= X^2\bar{p}^2\triangle - 2X\{2\bar{e}_2\beta\bar{p}^2 + (\bar{j}_2 + \bar{e}_3)(\alpha\bar{e}_2 - \beta\bar{d}_2)\bar{p} - 2\bar{e}_2\bar{j}_3\bar{d}_2\alpha\} \\ &\quad + 4\bar{k}_2\bar{f}_3\bar{e}_2\{\bar{j}_3\bar{d}_2^2 - (\bar{j}_2 + \bar{e}_3)\bar{p}\bar{d}_2 + \bar{e}_2\bar{p}^2\} \\ &\quad - (\alpha\bar{e}_2 + \beta\bar{d}_2)^2 \\ &= 0 \; . \qquad (12) \end{aligned}$$

Hence the values of $\bar{p}$ and $\bar{d}_2$ for which $X_{\max.} = \bar{f}_2$ are given by

$$S(\bar{f}_2, \bar{p}, \bar{d}_2) = 0 \; , \qquad (13)$$

which represents a conic section in the $(\bar{p}, \bar{d}_2)$ plane. The equation to the curve can be expressed in a form similar to (5), but the general expressions for the coefficients are complicated and will be omitted. In numerical cases the conic, which is found to be hyperbolic, can be constructed directly from (12) and (13).

It will now be shown that the upper branch B_u of the hyperbola can be taken as the stability boundary. The proof is similar to that given for flexural-aileron flutter. In Fig. 4, let N_1N be the chord through N parallel to OY. Then†

$$\frac{2\bar{j}_3B(Y_N - Y_{N1})}{q_1} = (\beta + \Omega)(\bar{j}_2 + \bar{e}_3)\bar{p} + 2\bar{j}_3(\alpha\bar{e}_2 - \Omega\bar{d}_2) \; ,$$

where B and q_1 are positive quantities. Hence N_1 lies below or above N according as

$$W(\bar{p}, \bar{d}_2) \equiv (\beta + \Omega)(\bar{j}_2 + \bar{e}_3)\bar{p} + 2\bar{j}_3(\alpha\bar{e}_2 - \Omega\bar{d}_2) < 0 \text{ or } > 0 \; .$$

But when N_1 coincides with N, the tangent at N is vertical, so that $X_{\max.} = X_N < \bar{f}_2$. It follows that the straight line $W = 0$ in the $(\bar{p}, \bar{d}_2)$ plane necessarily lies wholly between the branches of the hyperbola (13). Moreover, all points below the line yield test conics for which N_1 lies below N. But with such conics (*e.g.*, curve No. 2 of Fig. 4) flutter is prevented absolutely even when $X_{\max.} > \bar{f}_2$, provided Z lies above MN and to the right of N, as is assumed. Hence the region of the mass-balancing diagram which is below B_l can be included as safe.

Fig. 5 indicates the type of mass-balancing diagram to be expected. The gradient of the steeper asymptote will usually be slightly greater than unity and the centre C will be close to the origin. Thus the stability boundary B_u will be approximately represented by the straight line of unit gradient through the origin. In practice the constants n and N in Table 3 are small, so that both $\bar{p}$ and $\bar{d}_2$ will not differ greatly from g_3 (namely the true moment of inertia of the tab or servo). Hence any inertia point will lie close to the stability boundary.

Suppose $J_0(\bar{p}_0, \bar{d}_{20})$ in Fig. 5 to correspond to any datum inertial condition and to $\rho = \rho_0$. Then if a mass m is added to the flap (tab or servo) at distance λ forward of the flap hinge axis, and if D denotes the distance separating the two hinge axes of the system, the changes of the true inertias are

$$\delta d_2 = m\lambda^2 ; \qquad \delta p = -m\lambda(D - \lambda) ; \qquad \delta g_3 = m(D - \lambda)^2 .$$

Hence by Table 3

$$\delta\bar{p} = m\{\lambda n - (D - \lambda)\}\{\lambda N - (D - \lambda)\} ,$$

$$\delta\bar{d}_2 = m\{\lambda N - (D - \lambda)\}^2 .$$

The changes will certainly be beneficial provided the displacement of J_0 is towards the right and has a gradient less than unity. These conditions require, first, that $\delta\bar{p} > 0$, or

$$\{\lambda(n + 1) - D\}\{\lambda(N + 1) - D\} > 0 .$$

* *See* equation (152) of R. & M. 1155.

† *See* equation (150) of R. & M. 1155.

Hence m must lie outside the two limiting positions defined by $\lambda = D/(n + 1)$ and $\lambda = D/(\mathrm{N} + 1)$.

The second requirement is $\delta\bar{p} > \delta\bar{d}_2$, or

$$\{\lambda(n + 1) - D\}\{\lambda(\mathrm{N} + 1) - D\} - \{\lambda(\mathrm{N} + 1) - D\}^2 > 0 .$$

Thus

$$\lambda\{\lambda(\mathrm{N} + 1) - D\}(n - \mathrm{N}) > 0 .$$

When as normally $\mathrm{N} > n$, the condition becomes

$$\lambda(\mathrm{N} + 1) - D < 0 .$$

Hence, finally m must be placed at the right of the limiting position $\lambda = D/(\mathrm{N} + 1)$. This generalizes recommendation (C) given in section 16 of A.R.C. 5668, which was restricted to the special type of spring tab for which $n = 0$. The conclusion reached is independent of the flying height.

Numerical Example.—The following values for the barred coefficients relate to binary servo-rudder on a particular full-scale aircraft, and are calculated from data given in section 17 of A.R.C. 5668. The gearing constants are assumed to be $n = 0$ and $\mathrm{N} = 2\cdot73$.

$$\bar{e}_2 = 1\cdot17 , \quad \bar{f}_2 = 0\cdot344 , \quad \bar{j}_2 = 0\cdot868 , \quad \bar{k}_2 = 0\cdot0756 .$$

$$\bar{e}_3 = 1\cdot045 , \quad \bar{f}_3 = 0\cdot312 , \quad \bar{j}_3 = 0\cdot800 , \quad \bar{k}_3 = 0\cdot072 .$$

These yield

$$\beta = 0\cdot35007 , \quad \Omega = 0\cdot1843 , \quad \alpha = 0\cdot03095 - 0\cdot3877\bar{p} ,$$

$$X_M = 0\cdot1036 , \quad \mathrm{X_N} = 0\cdot3340 ,$$

$$\mathrm{Y}_M = 0\cdot2277 , \quad \mathrm{Y_N} = 0\cdot07062 .$$

The point Z $(0\cdot344, 0\cdot072)$ thus lies close above, and to the right of, N $(0\cdot334, 0\cdot0706)$.

Equation (13) reduces to

$$0\cdot03229\bar{p}^2 - 0\cdot06671\bar{p}\bar{d}_2 + 0\cdot03397\bar{d}_2^2 + 0\cdot01478\bar{p} - 0\cdot01456\bar{d}_2 + 0\cdot0013194 = 0 .$$

which represents a flat hyperbola (Fig. 6). The centre is at $\bar{p}_c = 0\cdot518$, $\bar{d}_2 = 0\cdot723$, and the gradients of the two asymptotes are $1\cdot10$ and $0\cdot865$. The stability boundary (upper branch) is practically indistinguishable from the steeper asymptote, and agrees closely with the linear stability boundary obtained by another method in section 17 of A.R.C. 5668, and shown in Fig. 17 of that report.

The two inertia points J_0, J_0' marked in Fig. 6 are both appropriate to a dynamically balanced servo-flap and to flight at sea level. They correspond to the following inertia values taken from Table B of section 17 of A.R.C. 5668 :—

(J_0) Balancing arm $\lambda = 6$ in., $\bar{d}_2 = 7\cdot667$, $\bar{p} = 7\cdot047$.

(J_0') Balancing arm $\lambda = 10\cdot2$ in., $\bar{d}_2 = 7\cdot488$, $\bar{p} = 6\cdot525$.

The critical length of arm in the case taken is

$$D/(N + 1) = 9\cdot26 \text{ in.}$$

REFERENCES

No.	*Author.*	*Title, etc.*
1	R. A. Frazer and W. P. Jones	Wing-Aileron-Tab Flutter. A.R.C. 5668. March, 1942. (To be published).
2	R. A. Frazer and W. J. Duncan.. ..	The Flutter of Aeroplane Wings. R. & M. 1155. August, 1928.
3	R. C. Pankhurst and J. F. C. Conn ..	Physical Properties of the Standard Atmosphere. R. & M. 1891. January, 1941.

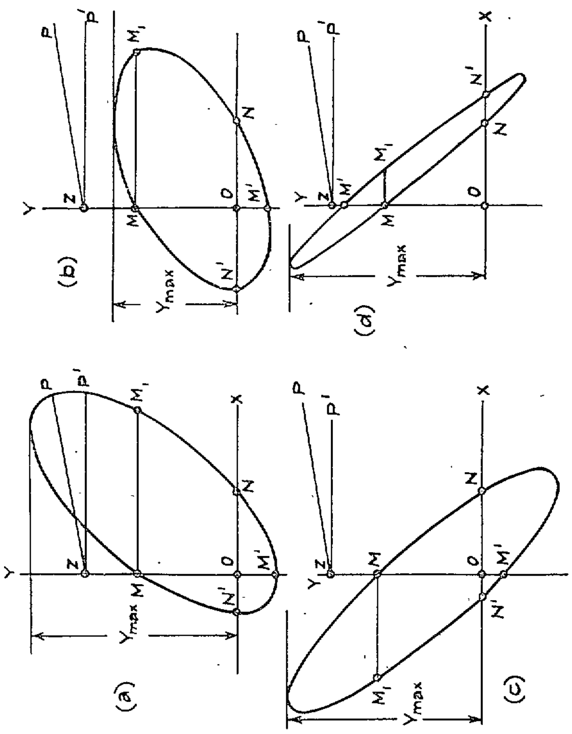

FIG. 1. Flexural-aileron Test Conics.

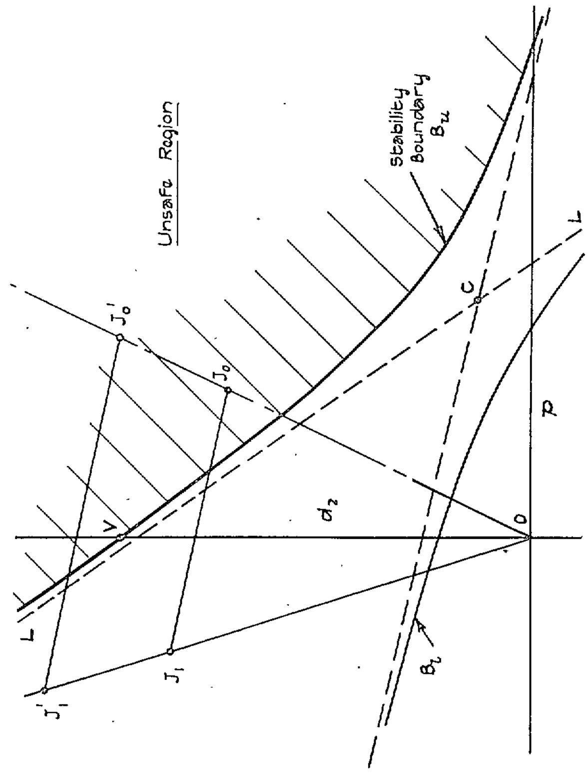

FIG. 2. Flexural-aileron Mass Balancing Diagram.

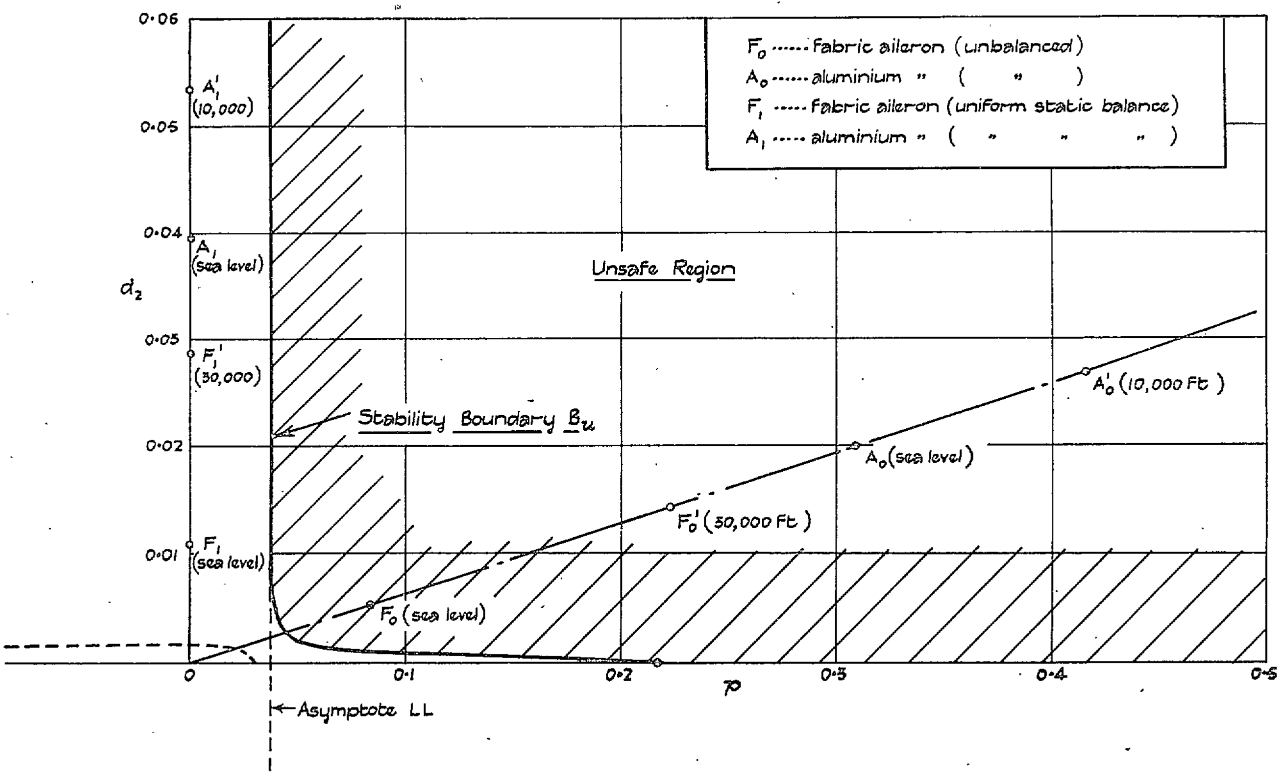

FIG. 3. Flexural-aileron Mass-balancing Diagram for Fighter Aircraft.

(93005) Wt. 13/806 K.5 12/50 Hw.

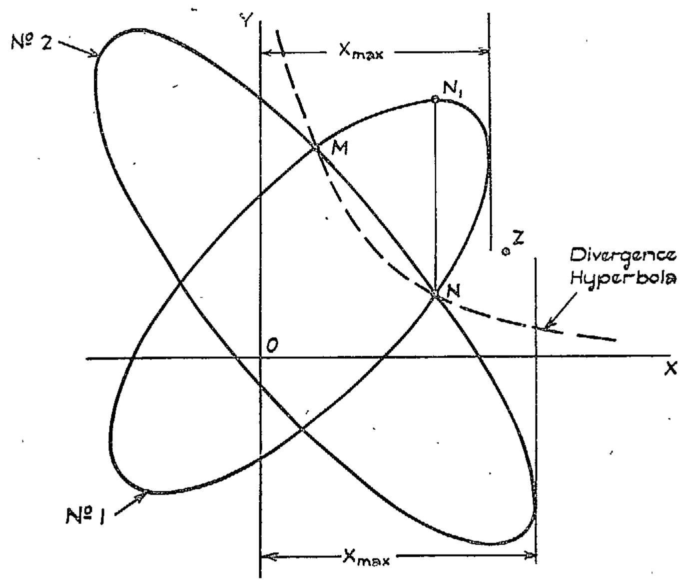

FIG. 4. Aileron-Tab, or Servo-rudder, Test Conics.

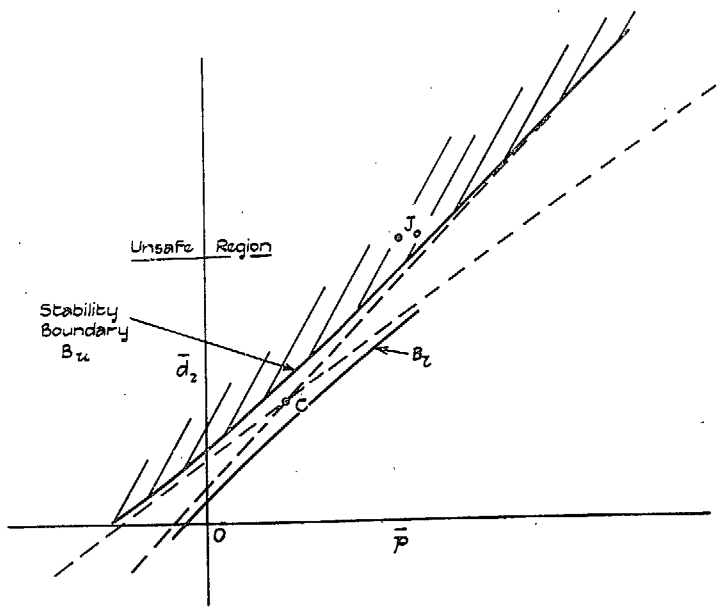

FIG. 5. Aileron-Tab, or Servo-rudder, Mass-balancing Diagram.

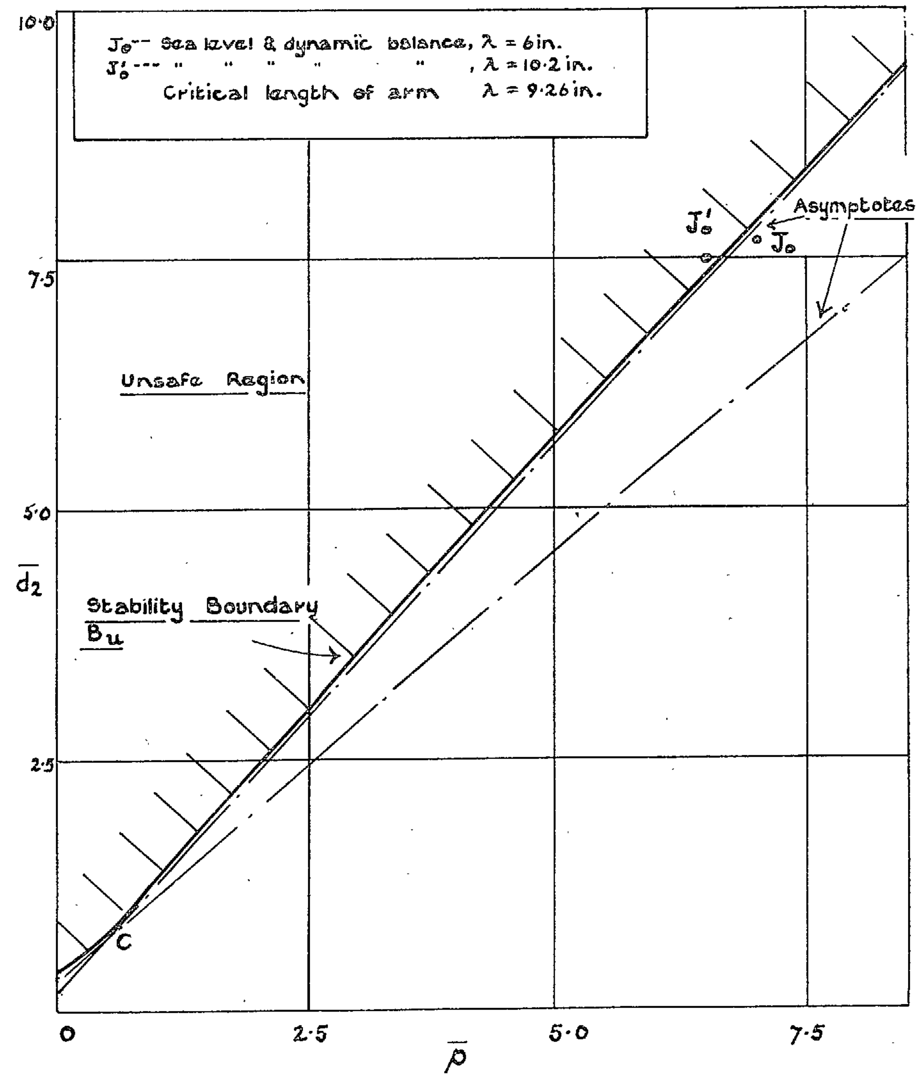

FIG. 6. Servo-rudder Mass-balancing Diagram for a Particular Aircraft.

PRINTED IN GREAT BRITAIN

Publications of the Aeronautical Research Committee

TECHNICAL REPORTS OF THE AERONAUTICAL RESEARCH COMMITTEE—

1934–35 Vol. I. Aerodynamics. 40*s.* (40*s.* 8*d.*)
Vol. II. Seaplanes, Structures, Engines, Materials, etc. 40*s.* (40*s.* 8*d.*)

1935–36 Vol. I. Aerodynamics. 30*s.* (30*s.* 7*d.*)
Vol. II. Structures, Flutter, Engines, Seaplanes, etc. 30*s.* (30*s.* 7*d.*)

1936 Vol. I. Aerodynamics General, Performance, Airscrews, Flutter and Spinning. 40*s.* (40*s.* 9*d.*)
Vol. II. Stability and Control, Structures, Seaplanes, Engines, etc. 50*s.* (50*s.* 10*d.*)

1937 Vol. I. Aerodynamics General, Performance, Airscrews, Flutter and Spinning. 40*s.* (40*s.* 9*d.*)
Vol. II. Stability and Control, Structures, Seaplanes, Engines, etc. 60*s.* (61*s.*)

1938 Vol. I. Aerodynamics General, Performance, Airscrews, 50*s.* (51*s.*)
Vol. II. Stability and Control, Flutter, Structures, Seaplanes, Wind Tunnels, Materials. 30*s.* (30*s.* 9*d.*)

1939 Vol. I. Aerodynamics General, Performance, Airscrews, Engines. 50*s.* (50*s.* 11*d.*)
Vol. II. Stability and Control, Flutter and Vibration, Instruments, Structures, Seaplanes, etc. 63*s.* (64*s.* 2*d.*)

ANNUAL REPORTS OF THE AERONAUTICAL RESEARCH COMMITTEE—

1933–34	1*s.* 6*d.* (1*s.* 8*d.*)
1934–35	1*s.* 6*d.* (1*s.* 8*d.*)
April 1, 1935 to December 31, 1936.	4*s.* (4*s.* 4*d.*)
1937	2*s.* (2*s.* 2*d.*)
1938	1*s.* 6*d.* (1*s.* 8*d.*)
1939-48	*In the press*

INDEXES TO THE TECHNICAL REPORTS OF THE ADVISORY COMMITTEE ON AERONAUTICS—

December 1, 1936 — June 30, 1939.	R. & M. No. 1850.	1*s.* 3*d.* (1*s.* 5*d.*)
July 1, 1939 — June 30, 1945.	R. & M. No. 1950.	1*s.* (1*s.* 2*d.*)
July 1, 1945 — June 30, 1946.	R. & M. No. 2050.	1*s.* (1*s.* 1*d.*)
July 1, 1946 — December 31, 1946.	R. & M. No. 2150.	1*s.* 3*d.* (1*s.* 4*d.*)
January 1, 1947 — June 30, 1947.	R. & M. No. 2250.	1*s.* 3*d.* (1*s.* 4*d.*)

Prices in brackets include postage.

Obtainable from

His Majesty's Stationery Office

York House, Kingsway, LONDON, W.C.2   429 Oxford Street, LONDON, W.1
P.O. Box 569, LONDON, S.E.1
13a Castle Street, EDINBURGH, 2   1 St. Andrew's Crescent, CARDIFF
39 King Street, MANCHESTER, 2   Tower Lane, BRISTOL, 1
2 Edmund Street, BIRMINGHAM, 3   80 Chichester Street, BELFAST

or through any bookseller.

S.O. Code No. 23-2551